

Cell Reports, Volume 34

Supplemental Information

G α is a major determinant of cAMP signaling in the pathophysiology of movement disorders

Brian S. Muntean, Ikuo Masuho, Maria Dao, Laurie P. Sutton, Stefano Zucca, Hideki Iwamoto, Dipak N. Patil, Dandan Wang, Lutz Birnbaumer, Randy D. Blakely, Brock Grill, and Kirill A. Martemyanov

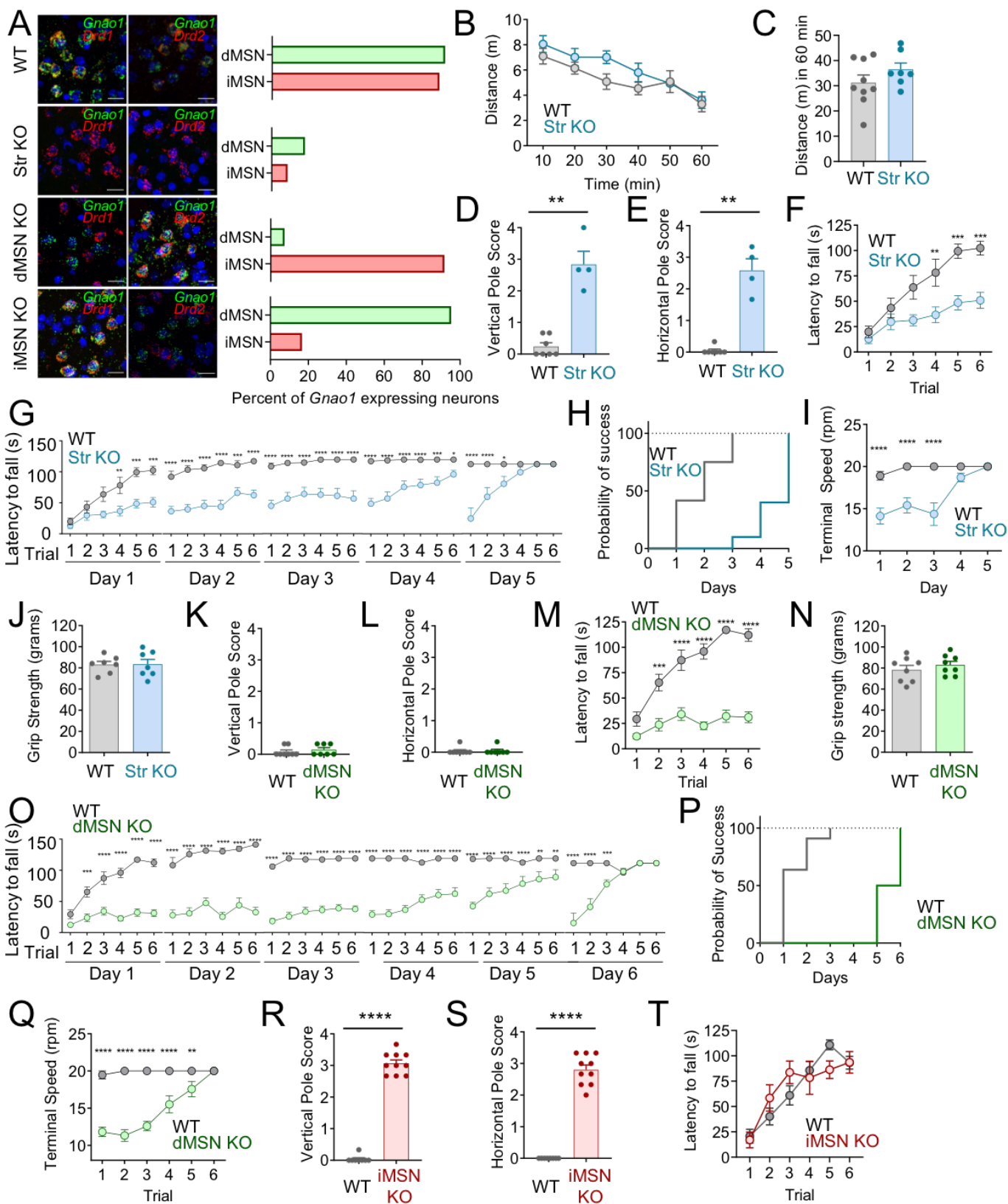


Figure S1. Related to Figure 1. Characterization of motor behavior in mice with striatal specific elimination of $G\alpha_o$.

A) *In situ* hybridization showing expression of *Gnao1* mRNA in dMSN (*Drd1* mRNA) and iMSN (*Drd2* mRNA) in the dorsal striatum of adult WT (*Gnao1^{flox/flox}*; n=4 mice), Str KO (*Gnao1^{flox/flox}:RGS9^{Cre}*; n=2 mice), dMSN KO (*Gnao1^{flox/flox}:Drd1a^{Cre}*; n=2 mice), and iMSN KO (*Gnao1^{flox/flox}:Drd2^{Cre}*; n=2 mice). Quantification of percent of *Gnao1* expressing dMSNs or iMSNs. **B)** Time course in the open field assay. *Gnao1^{flox/flox}* (WT; n=9) and *Gnao1^{flox/flox}:RGS9^{Cre}* (Str KO; n=8). **C)** Total distance traveled in the open field assay. *Gnao1^{flox/flox}* (WT; n=9) and *Gnao1^{flox/flox}:RGS9^{Cre}* (Str KO; n=8), nonparametric t-test p=0.4302, Kolmogorov-Smirnov D=0.4127. **D)** Vertical pole assay pathology score for *Gnao1^{flox/flox}* (WT; n=7) and *Gnao1^{flox/flox}:RGS9^{Cre}* (Str KO; n=4) mice. Nonparametric t-test p=0.0061, Kolmogorov-Smirnov D=1.000. **E)** Horizontal pole assay pathology score for *Gnao1^{flox/flox}* (WT; n=7) and *Gnao1^{flox/flox}:RGS9^{Cre}* (Str KO; n=4) mice. Nonparametric t-test p=0.0030, Kolmogorov-Smirnov D=1.000. **F)** Performance of *Gnao1^{flox/flox}* (WT; n=12) and *Gnao1^{flox/flox}:RGS9^{Cre}* (Str KO; n=10) littermates on intraday intervals on the accelerating rotarod. Two-way ANOVA, Bonferroni's multiple comparisons test. **G)** Daily performance of *Gnao1^{flox/flox}* (WT; n=12) and *Gnao1^{flox/flox}:RGS9^{Cre}* (Str KO; n=10) mice on the accelerating rotarod over 5 days (6 trials/day). Two-way ANOVA, Bonferroni's multiple comparisons test. **H)** Probability of reaching maximal speed over 5 days of training on the accelerating rotarod for *Gnao1^{flox/flox}* (WT; n=12) and *Gnao1^{flox/flox}:RGS9^{Cre}* (Str KO; n=10) mice. **I)** Time course of the terminal speed over 5 consecutive training days on the accelerating rotarod for *Gnao1^{flox/flox}* (WT; n=12) and *Gnao1^{flox/flox}:RGS9^{Cre}* (Str KO; n=10) mice. Two-way ANOVA, Bonferroni's multiple comparisons test. **J)** Grip strength for *Gnao1^{flox/flox}* (WT; n=7) and *Gnao1^{flox/flox}:RGS9^{Cre}* (Str KO; n=7) mice, nonparametric t-test p=0.9627, Kolmogorov-Smirnov D=0.2857. **K)** Vertical pole assay pathology score for *Gnao1^{flox/flox}* (WT; n=8) and *Gnao1^{flox/flox}:Drd1a^{Cre}* (dMSN KO; n=7) mice. Nonparametric t-test p=0.6084, Kolmogorov-Smirnov D=0.1786. **L)** Horizontal pole assay pathology score for *Gnao1^{flox/flox}* (WT; n=8) and *Gnao1^{flox/flox}:Drd1a^{Cre}* (dMSN KO; n=7) mice. Nonparametric t-test p>0.9999, Kolmogorov-Smirnov D=0.01786. **M)** Performance of *Gnao1^{flox/flox}* (WT; n=11) and *Gnao1^{flox/flox}:Drd1a^{Cre}* (dMSN KO; n=8) littermates on intraday intervals on the accelerating rotarod. Two-way ANOVA, Bonferroni's multiple comparisons test. **N)** Grip strength for *Gnao1^{flox/flox}* (WT; n=8) and *Gnao1^{flox/flox}:Drd1a^{Cre}* (dMSN KO; n=8) mice, nonparametric t-test p=0.6601, Kolmogorov-Smirnov D=0.3750. **O)** Daily performance of *Gnao1^{flox/flox}* (WT; n=11) and *Gnao1^{flox/flox}:Drd1a^{Cre}* (dMSN KO; n=8) mice on the accelerating rotarod over 6 days (6 trials/day). Two-way ANOVA, Bonferroni's multiple comparisons test. **P)** Probability of reaching maximal speed over 6 days of training on the accelerating rotarod for *Gnao1^{flox/flox}* (WT; n=11) and *Gnao1^{flox/flox}:Drd1a^{Cre}* (dMSN KO; n=8) mice. **Q)** Time course of the terminal speed over 6 consecutive training days on the accelerating rotarod for *Gnao1^{flox/flox}* (WT; n=11) and *Gnao1^{flox/flox}:Drd1a^{Cre}* (dMSN KO; n=8) mice. Two-way ANOVA, Bonferroni's multiple comparisons test. **R)** Vertical pole assay pathology score for *Gnao1^{flox/flox}* (WT; n=8) and *Gnao1^{flox/flox}:Drd2^{Cre}* (iMSN KO; n=10) mice. Nonparametric t-test p<0.0001, Kolmogorov-Smirnov D=1.000. **S)** Horizontal pole assay pathology score for *Gnao1^{flox/flox}* (WT; n=8) and *Gnao1^{flox/flox}:Drd2^{Cre}* (iMSN KO; n=10) mice. Nonparametric t-test p<0.0001, Kolmogorov-Smirnov D=1.000. **T)** Performance of *Gnao1^{flox/flox}* (WT; n=8) and *Gnao1^{flox/flox}:Drd2^{Cre}* (iMSN KO; n=7) littermates on intraday intervals on the accelerating rotarod. Two-way ANOVA, Bonferroni's multiple comparisons test. All data are represented as mean \pm SEM; *p < 0.05; **p < 0.01; *** p < 0.001; **** p < 0.0001.

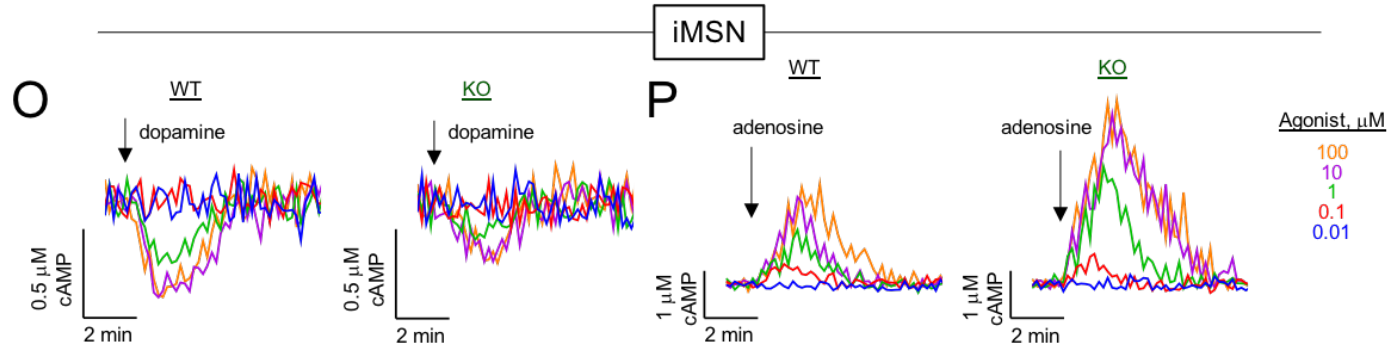
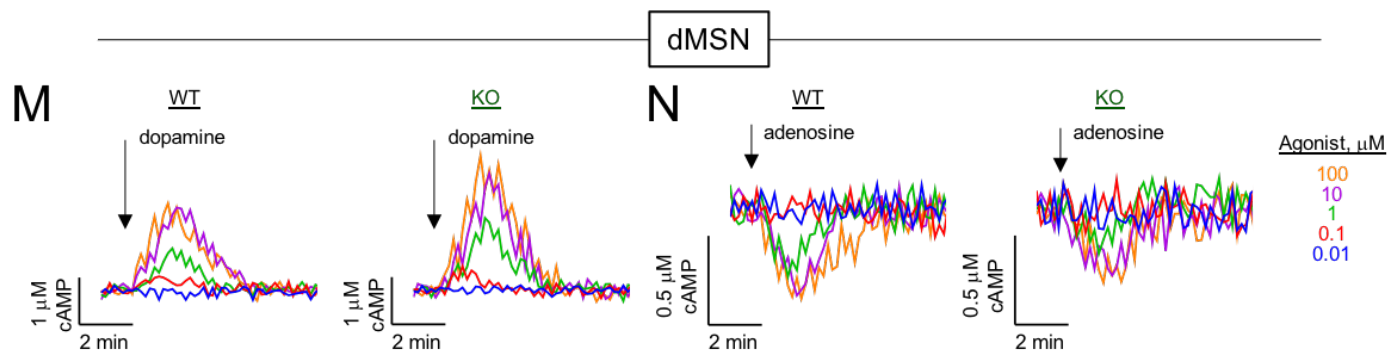
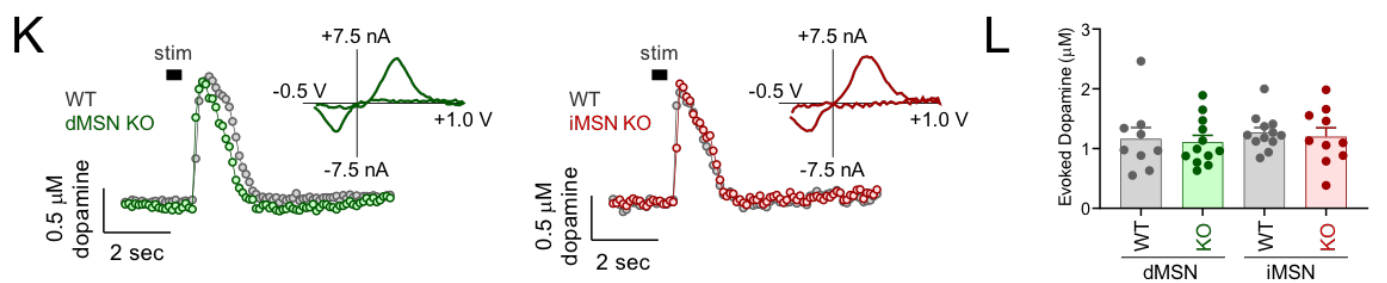
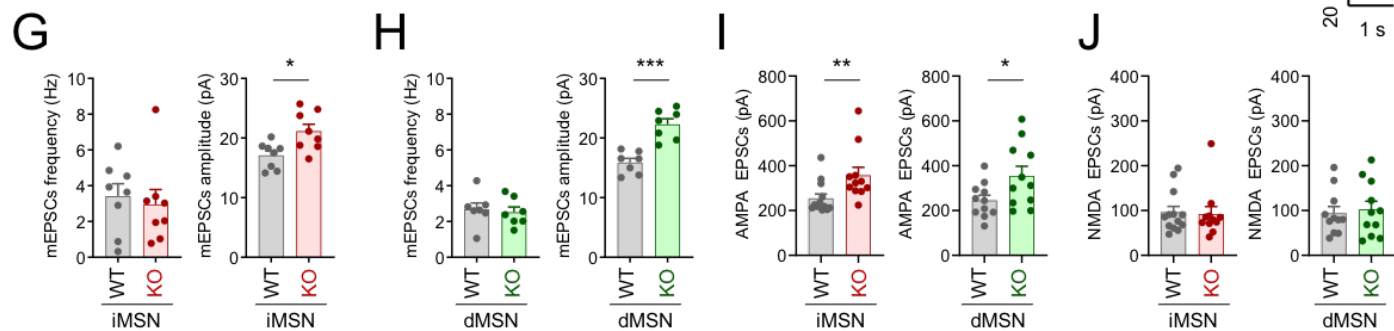
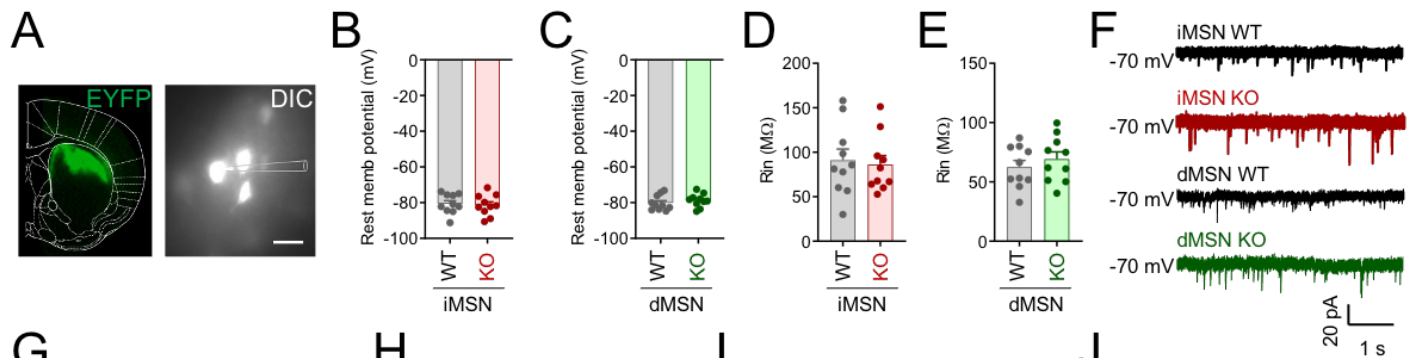


Figure S2. Related to Figure 2. Characterization *Gnao1* inactivation in striatal neurons. **A)** Coronal striatal section (100 μm) showing viral expression of EYFP targeted to dorsal striatum (left) and DIC image showing identification of EYFP MSNs in a coronal slice (300 μm) for electrophysiological recordings (right). **B)** Resting membrane potential of acute brain slice iMSNs from *Drd2^{Cre}* (WT; n=7 mice/10 neurons) and *Gnao1^{fllox/fllox}:Drd2^{Cre}* (iMSN KO; n=5 mice/10 neurons). Nonparametric t-test; Mann-Whitney test, p=0.7394. **C)** Resting membrane potential of acute brain slice dMSNs from *Drd1a^{Cre}* (WT; n=7 mice/10 neurons) and *Gnao1^{fllox/fllox}:Drd1a^{Cre}* (dMSN KO; n=6 mice/10 neurons). Nonparametric t-test; Mann-Whitney test, p=0.3930. **D)** Input resistance of acute brain slice iMSNs from *Drd2^{Cre}* (WT; n=7 mice/10 neurons) and *Gnao1^{fllox/fllox}:Drd2^{Cre}* (iMSN KO; n=5 mice/10 neurons). Nonparametric t-test; Mann-Whitney test, p=0.7959. **E)** Input resistance of acute brain slice dMSNs from *Drd1a^{Cre}* (WT; n=7 mice/10 neurons) and *Gnao1^{fllox/fllox}:Drd1a^{Cre}* (dMSN KO; n=6 mice/10 neurons). Nonparametric t-test; Mann-Whitney test, p=0.6305. **F)** Representative mEPSCs traces from the dorsal striatum of acute coronal brain slices. **G)** Quantification of iMSN mEPSCs frequency (nonparametric t-test; Mann-Whitney test, p=0.4418) and amplitude (nonparametric t-test; Mann-Whitney test, p=0.0148). (WT; n=4 mice/8 neurons; iMSN KO; n=3 mice/8 neurons). **H)** Quantification of dMSN mEPSCs frequency (nonparametric t-test; Mann-Whitney test, p=0.4557) and amplitude (nonparametric t-test; Mann-Whitney test, p=0.0006). (WT; n=3 mice/7 neurons; dMSN KO; n=3 mice/7 neurons). **I)** Quantification of AMPA EPSCs amplitude from *Drd2^{Cre}* (WT; n=6 mice/13 neurons) and *Gnao1^{fllox/fllox}:Drd2^{Cre}* (iMSN KO; n=6 mice/11 neurons). Nonparametric t-test; Mann-Whitney test, p=0.0048. Quantification of AMPA EPSCs amplitude from *Drd1a^{Cre}* (WT; n=6 mice/11 neurons) and *Gnao1^{fllox/fllox}:Drd1a^{Cre}* (dMSN KO; n=5 mice/11 neurons). Nonparametric t-test; Mann-Whitney test, p=0.0473. **J)** Quantification of NMDA EPSCs amplitude from *Drd2^{Cre}* (WT; n=6 mice/13 neurons) and *Gnao1^{fllox/fllox}:Drd2^{Cre}* (iMSN KO; n=6 mice/11 neurons). Nonparametric t-test; Mann-Whitney test, p=0.6905. Quantification of NMDA EPSCs amplitude from *Drd1a^{Cre}* (WT; n=6 mice/11 neurons) and *Gnao1^{fllox/fllox}:Drd1a^{Cre}* (dMSN KO; n=5 mice/11 neurons). Nonparametric t-test; Mann-Whitney test, p=0.9487. **K)** Representative traces of fast scan cyclic voltammetry (FSCV) and triangular waveform measuring evoked dopamine in response to electrical stimulation from the dorsal striatum of acute coronal brain slices. **L)** Quantification of evoked dopamine between dMSN WT (2 animals, 9 slices), dMSN KO (2 animals, 12 slices), iMSN WT (2 animals, 12 slices), and iMSN KO (2 animals, 9 slices). **M)** Representative traces of dopamine-induced cAMP responses in dMSNs from *Gnao1^{fllox/fllox}* (WT) and *Gnao1^{fllox/fllox}:RGS9^{Cre}* (dMSN KO). **N)** Representative traces of adenosine-induced cAMP responses in dMSNs from *Gnao1^{fllox/fllox}* (WT) and *Gnao1^{fllox/fllox}:RGS9^{Cre}* (dMSN KO). **O)** Representative traces of dopamine-induced cAMP responses in iMSNs from *Gnao1^{fllox/fllox}* (WT) and *Gnao1^{fllox/fllox}:RGS9^{Cre}* (iMSN KO). **P)** Representative traces of adenosine-induced cAMP responses in iMSNs from *Gnao1^{fllox/fllox}* (WT) and *Gnao1^{fllox/fllox}:RGS9^{Cre}* (iMSN KO). All data are represented as mean \pm SEM; *p < 0.05; **p < 0.01; *** p < 0.001; **** p < 0.0001.

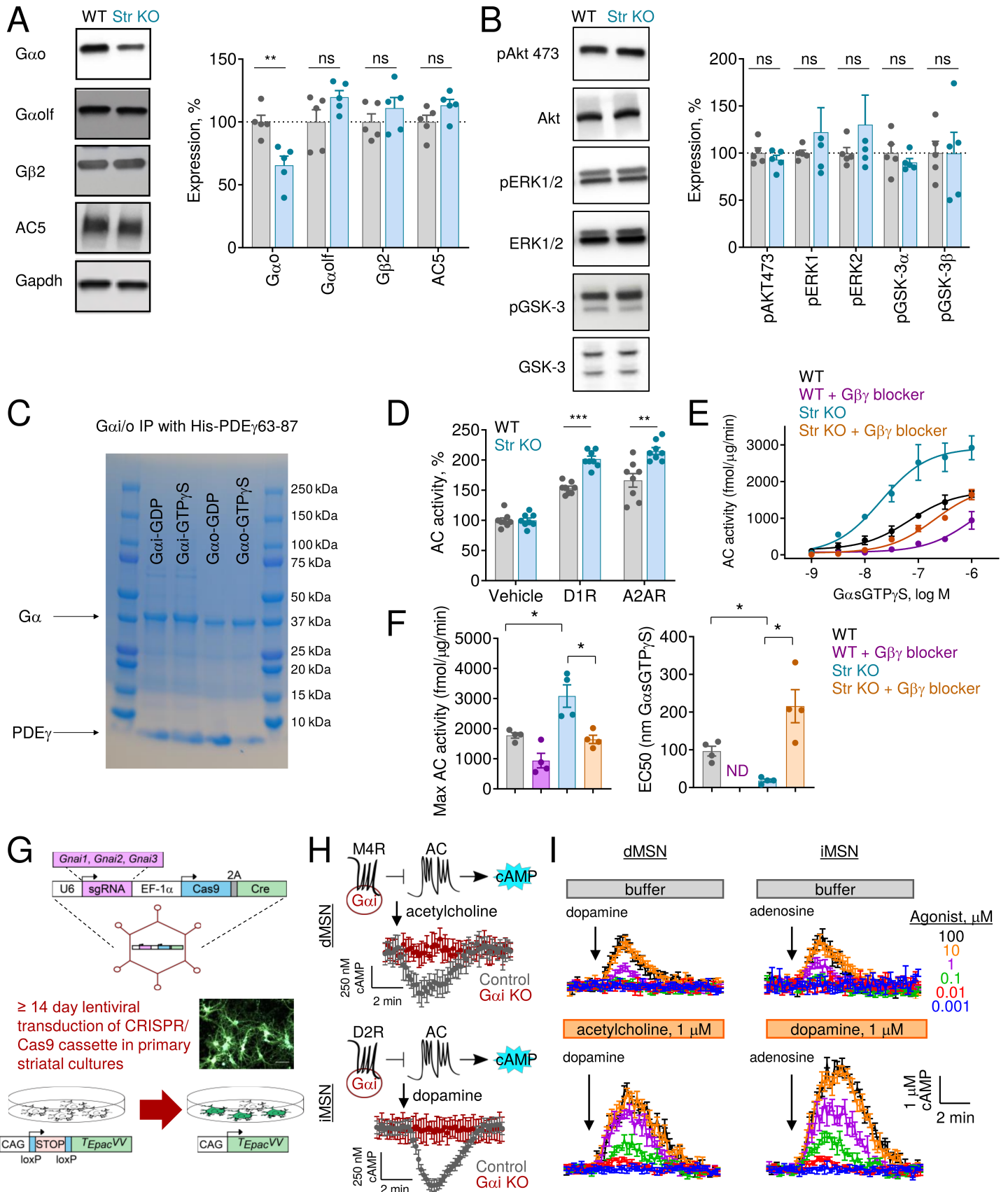


Figure S3. Related to Figure 3. Biochemical characterization of striatal tissues lacking *Gαo*.

A) Western blot analysis of striatal tissue punches from *Gnao1^{fllox/fllox}* (WT; n=5) and *Gnao1^{fllox/fllox}:RGS9^{Cre}* (Str KO; n=5) mice to examine *Gαo* (nonparametric t-test; Mann-Whitney test, p=0.0079), *Gαolf* (nonparametric t-test; Mann-Whitney test, p=0.2222), *Gβ2* (nonparametric t-test; Mann-Whitney test, p=0.2698), and *AC5* (nonparametric t-test; Mann-Whitney test, p=0.0952). **B)** Western blot analysis of striatal tissue punches from *Gnao1^{fllox/fllox}* (WT; n=5) and *Gnao1^{fllox/fllox}:RGS9^{Cre}* (Str KO; n=5) mice to examine pAKT 473 (nonparametric t-test; Mann-Whitney test, p=0.5476), pERK1 (nonparametric t-test; Mann-Whitney test, p=0.8413), pERK2 (nonparametric t-test; Mann-Whitney test, p=0.6905), pGSK-3α (nonparametric t-test; Mann-Whitney test, p=0.3095), and pGSK-3β (nonparametric t-test; Mann-Whitney test, p>0.9999). **C)** Representative coomassie gel of *in vitro* immunoprecipitation between recombinant fragment of PDEγ with *Gαi*-GDP, *Gαi*-GTPγS, *Gαo*-GDP, or *Gαo*-GTPγS (n=3). **D)** Efficacy of vehicle (p>0.9999), D1R agonist (10 μM SKF81297; p=0.0002) and A2AR agonist (10 μM CGS21680; p=0.0031) on striatal AC activity (n=8 experiments), nonparametric t-test; Mann-Whitney test. **E)** *Gαs*-GTPγS dose response on striatal membranes in presence of a *Gβγ* scavenger (Grk2i peptide). n=4 experiments. **F)** Efficacy of *Gαs*-GTPγS, WT vs Str KO (nonparametric t-test; Mann-Whitney test, p=0.0286); Str KO vs Str KO + *Gβγ* scavenger (nonparametric t-test; Mann-Whitney test, p=0.0286). EC50 to *Gαs*-GTPγS, WT vs Str KO (nonparametric t-test; Mann-Whitney test, p=0.0286); Str KO vs Str KO + *Gβγ* scavenger (nonparametric t-test; Mann-Whitney test, p=0.0286). n=4 experiments. **G)** Schematic of *Gαi* KO utilizing CRISPR/Cas9 in cAMP Encoded Reporter (CAMPER) primary striatal neurons to simultaneously express the ^TEpac^{VV} biosensor. **H)** Average traces of *Gαi* KO (n=9 neurons) or control (n=10 neurons) dMSN response to acetylcholine (top) and iMSN response to dopamine (n= 30 neurons/control; 26 neurons *Gαi* KO) (bottom). **I)** Average traces of dopamine-induced cAMP response in *Gαi* KO dMSNs in the presence (n≥6 neurons/dose) or absence of acetylcholine (n=10 neurons/dose) (left). Average traces of adenosine-induced cAMP response in *Gαi* KO iMSNs in the presence (n≥5 neurons/dose) or absence of dopamine (n=10 neurons/dose) (right). All data are represented as mean ± SEM; *p < 0.05; **p < 0.01; *** p < 0.001; **** p < 0.0001.

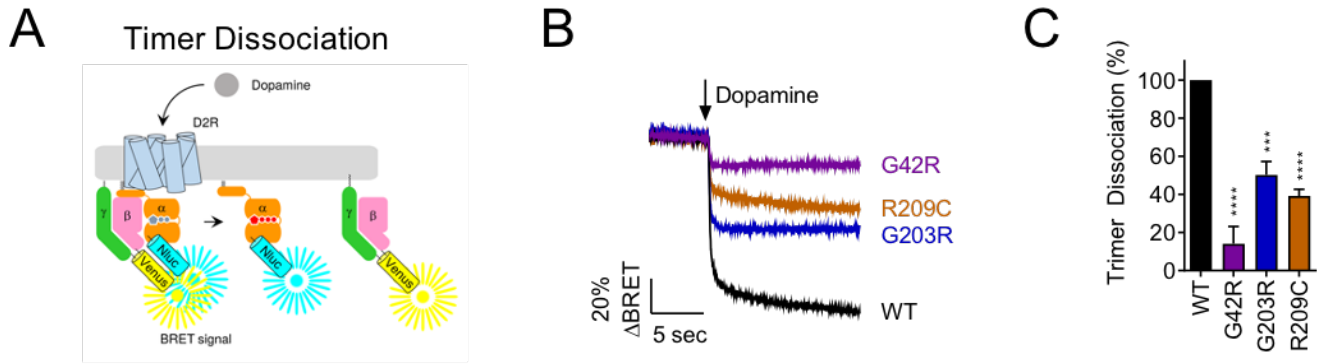


Figure S4. Related to Figure 4. Direct dissociation of Gαo and Gβγ subunits.

A) Assay design to monitor direct dissociation of Gαo from Gβγ. HEK293T/17 cells were transfected with plasmids encoding Flag-D2R, Gαo-Nluc, and Venus-Gβ1γ2. Dopamine application to the transfected cells induces dissociation of Gαo from Venus-Gβ1γ2, which decreases BRET ratio through loss of interaction with Venus-Gβ1γ2. **B)** Timecourse of agonist-mediated dissociation of Gαo and Venus-Gβ1γ2. **C)** Effect of mutations on trimer dissociation measured by change in BRET ratio. The ratio obtained with wild-type Gαo is designated as 100% trimer dissociation. The mean ± SEM of three independent experiments is shown in the bar graph. One-way ANOVA followed by Dunnett's multiple comparisons tests was conducted to determine the effect of genetic variants on the functions of Gαo with WT. *p < 0.05; **p < 0.01; *** p < 0.001; **** p < 0.0001.

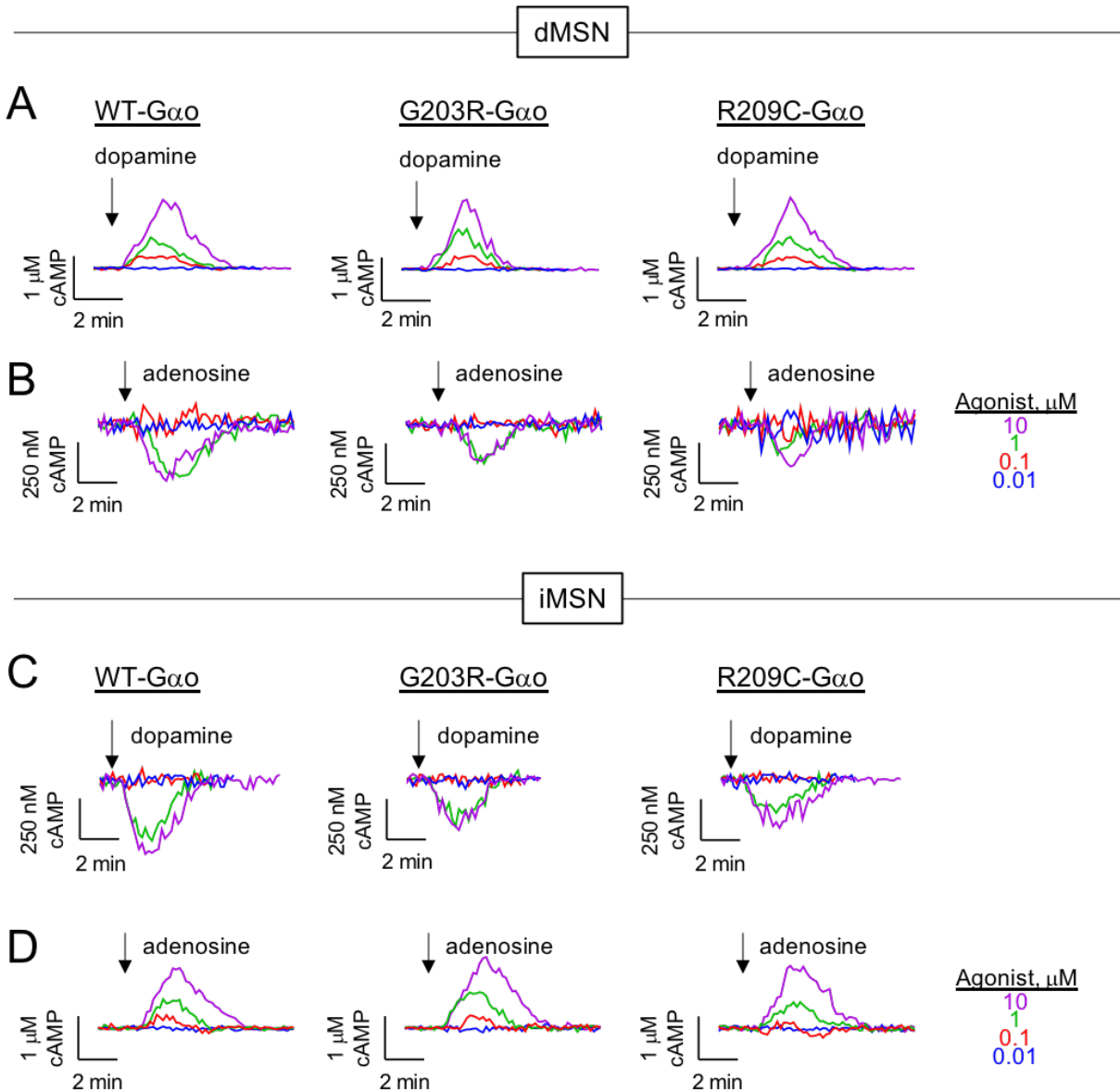


Figure S5. Related to Figure 5. *GNAO1* influence on dopamine and adenosine-mediated cAMP signaling in primary striatal neurons.

A) Average cAMP responses to dopamine dose response from *Gnao1^{lox/lox}* dMSNs transfected with the indicated G α o construct. n (# neurons)= No G α (13), WT G α o (10), G203R (8), R209C (10). **B)** Average cAMP responses to adenosine dose response from *Gnao1^{lox/lox}* dMSNs transfected with the indicated G α o construct. n (# neurons)= No G α (13), WT G α o (12), G203R (13), R209C (14). **C)** Average cAMP responses to dopamine dose response from *Gnao1^{lox/lox}* iMSNs transfected with the indicated G α o construct. n (# neurons)= No G α (12), WT G α o (6), G203R (8), R209C (7). **D)** Average cAMP responses to adenosine dose response from *Gnao1^{lox/lox}* iMSNs transfected with the indicated G α o construct. n (# neurons)= No G α (12), WT G α o (13), G203R (12), R209C (13).

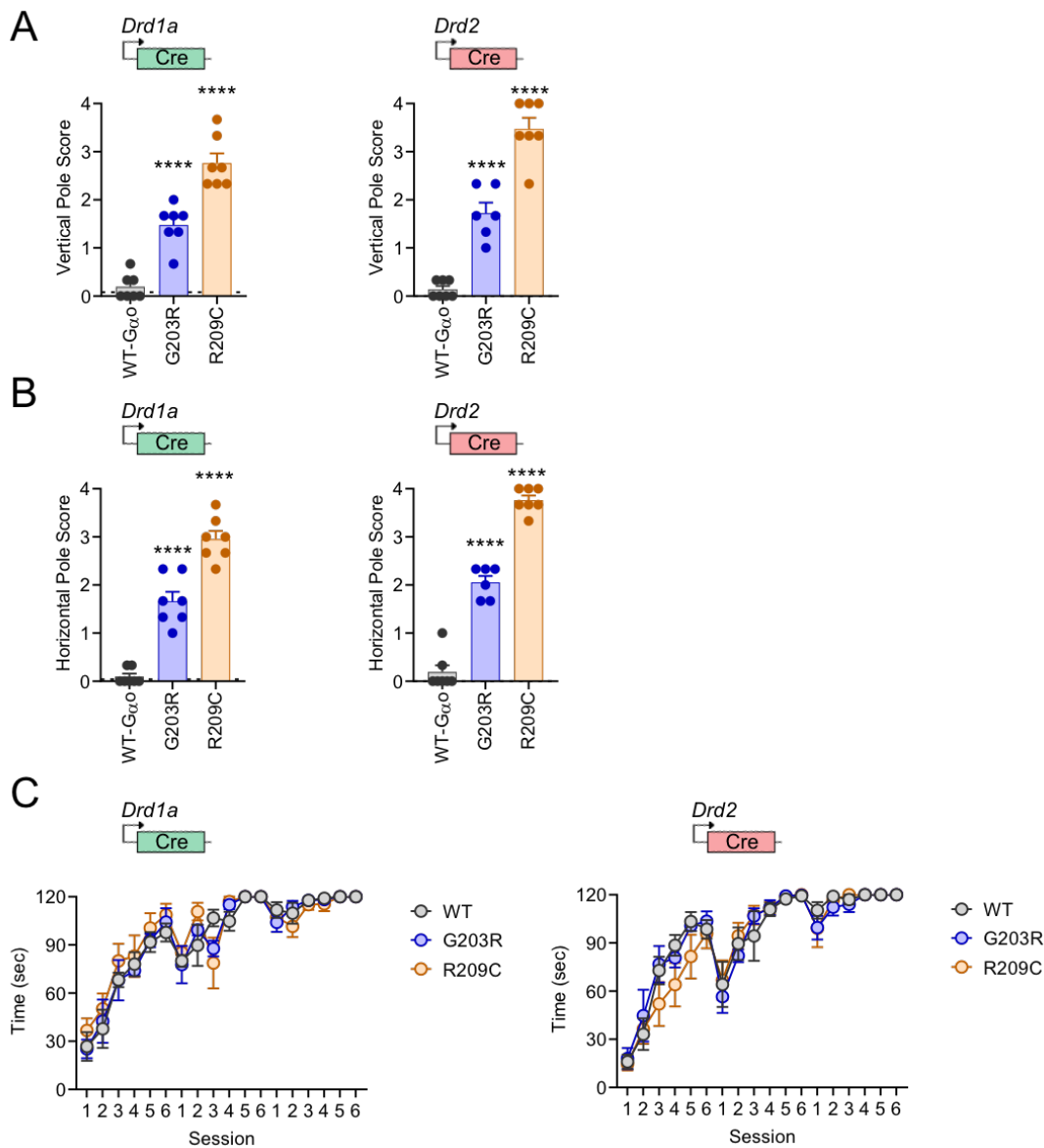


Figure S6. Related to Figure 6. Characterization of motor behavior in mice with striatal specific expression of GNAO1 clinical variants.

A) Vertical pole assay pathology score for *Drd1a*^{Cre} mice expressing WT Gαo (n=7), G203R Gαo (n=7), or R209C Gαo (n=7). One-way ANOVA, Dunnett's multiple comparisons test; WT vs G203R p<0.0001, WT vs R209C p<0.0001 (left). Vertical pole assay pathology score for *Drd2*^{Cre} mice expressing WT Gαo (n=7), G203R Gαo (n=6), or R209C Gαo (n=7). One-way ANOVA, Dunnett's multiple comparisons test; WT vs G203R p<0.0001, WT vs R209C p<0.0001 (right). **B)** Horizontal pole assay pathology score for *Drd1a*^{Cre} mice expressing WT Gαo (n=7), G203R Gαo (n=7), or R209C Gαo (n=7). One-way ANOVA, Dunnett's multiple comparisons test; WT vs G203R p<0.0001, WT vs R209C p<0.0001 (left). Horizontal pole assay pathology score for *Drd2*^{Cre} mice expressing WT Gαo (n=7), G203R Gαo (n=6), or R209C Gαo (n=7). One-way ANOVA, Dunnett's multiple comparisons test; WT vs G203R p<0.0001, WT vs R209C p<0.0001 (right). **C)** Daily performance on the accelerating rotarod over 3 days (6 trials/day) of *Drd1a*^{Cre} mice expressing WT Gαo (n=4), G203R Gαo (n=4), or R209C Gαo (n=4) and *Drd2*^{Cre} mice expressing WT Gαo (n=4), G203R Gαo (n=4), or R209C Gαo (n=4).

Table S1. Oligonucleotide information. Related to STAR Methods.

Name	Sequence
Gnai1 sgRNA 1 FW	5'-CACCGACGCTGCCGAATCGTTCAGC
Gnai1 sgRNA 1 RV	5'-AAACGCTGAACGATTCGGCAGCGTC
Gnai1 sgRNA 2 FW	5'-CACCGGGTAGGATTATCCACGAAGC
Gnai1 sgRNA 2 RV	5'-AAACGCTTCGTGGATAATCCTACCC
Gnai1 sgRNA 3 FW	5'-CACCGCTCCCGGGATCTGTTGAAGC
Gnai1 sgRNA 3 RV	5'-AAACGCTTCAACAGATCCCGGGAGC
Gnai2 sgRNA 1 FW	5'-CACCGGTGCCGGCAGTACCGTGCCG
Gnai2 sgRNA 1 RV	5'-AAACCGGCACGGTACTGCCGGCACC
Gnai2 sgRNA 2 FW	5'-CACCGAGGGCACGCACCGCACGCTG
Gnai2 sgRNA 2 RV	5'-AAACCAGCGTGCGGTGCGTGCCCTC
Gnai2 sgRNA 3 FW	5'-CACCGTTCTCGTGAGCGGCCAAAGC
Gnai2 sgRNA 3 RV	5'-AAACGCTTTGGCCGCTCACGAGAAC
Gnai3 sgRNA 1 FW	5'-CACCGCATTGCAATCATACGAGCCA
Gnai3 sgRNA 1 RV	5'-AAACTGGCTCGTATGATTGCAATGC
Gnai3 sgRNA 2 FW	5'-CACCGATCAATCTTCAACCGTCCCA
Gnai3 sgRNA 2 RV	5'-AAACTGGGACGGTTGAAGATTGATC
Gnai3 sgRNA 3 FW	5'-CACCGATTAAACGTTTATGGCGAGA
Gnai3 sgRNA 3 RV	5'-AAACTCTCGCCATAAACGTTTAATC

Table S2. F-test parameters for dose-response experiments.

Figure	Comparison	F (DFn, Dfd)	p value
2I	WT vs dMSN KO	4.321 (1, 132)	0.0396
2J	WT vs dMSN KO	0.1574 (1, 134)	0.6922
2K	WT vs IMSN KO	0.02787 (1, 117)	0.8677
2L	WT vs IMSN KO	2.038 (1, 117)	0.1561
3C	-Gbg vs +Gbg	1.613 (1, 113)	0.2067
3F	WT vs Str KO	18.41 (1, 138)	<0.0001
3L	buffer vs acetylcholine	27.10 (1, 95)	<0.0001
3Q	buffer vs dopamine	4.333 (1, 91)	0.0402
S3E	WT vs Str KO	2.672 (1, 50)	0.1084
S3E	Str KO vs Str KO +Gbg blocker	7.561 (1, 50)	0.0083
5B	WT Gao vs No Gao	0.1057 (1, 86)	0.7459
5B	WT Gao vs G203R Gao	8.968 (1, 66)	0.0039
5B	WT Gao vs R209C Gao	0.2986 (1, 74)	0.5864
5D	WT Gao vs No Gao	1.611 (1, 94)	0.2075
5D	WT Gao vs G203R Gao	0.02029 (1, 94)	0.887
5D	WT Gao vs R209C Gao	1.219 (1, 98)	0.2723
5F	WT Gao vs No Gao	1.091 (1, 66)	0.3001
5F	WT Gao vs G203R Gao	0.3727 (1, 50)	0.5443
5F	WT Gao vs R209C Gao	0.3380 (1, 46)	0.5638
5H	WT Gao vs No Gao	0.004690 (1, 94)	0.9455
5H	WT Gao vs G203R Gao	8.968 (1, 66)	0.0039
5H	WT Gao vs R209C Gao	0.006707 (1, 98)	0.9349